

## Dithiocarbamates Strongly Inhibit Carbonic Anhydrases and Show Antiglaucoma Action in Vivo

Fabrizio Carta,<sup>†</sup> Mayank Aggarwal,<sup>‡</sup> Alfonso Maresca,<sup>†</sup> Andrea Scozzafava,<sup>†</sup> Robert McKenna,<sup>‡</sup> Emanuela Masini,<sup>§</sup> and Claudiu T. Supuran<sup>\*,†</sup>

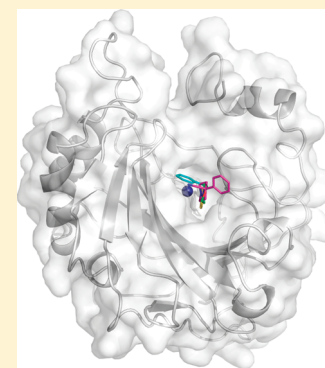
<sup>†</sup>Laboratorio di Chimica Bioinorganica, Polo Scientifico, Università degli Studi di Firenze, Room 188, Via della Lastruccia 3, 50019 Sesto Fiorentino, Florence, Italy

<sup>‡</sup>Department of Biochemistry and Molecular Biology, College of Medicine, University of Florida, Box 100245, Gainesville, Florida 32610, United States

<sup>§</sup>Department of Preclinical and Clinical Pharmacology, Università degli Studi di Firenze, Viale Pierracini 6, Florence, Italy

### **S** Supporting Information

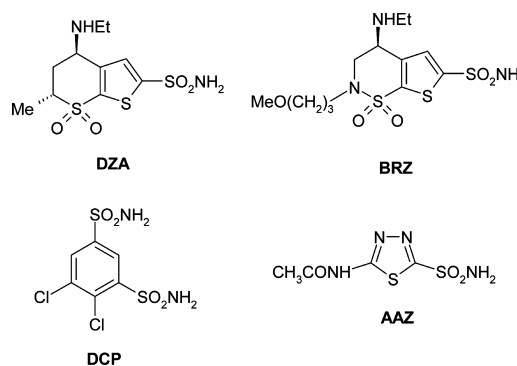
**ABSTRACT:** A series of dithiocarbamates were prepared by reaction of primary/secondary amines with carbon disulfide in the presence of bases. These compounds were tested for the inhibition of four human (h) isoforms of the zinc enzyme carbonic anhydrase, CA (EC 4.2.1.1), hCA I, II, IX, and XII, involved in pathologies such as glaucoma (CA II and XII) or cancer (CA IX). Several low nanomolar inhibitors targeting these CAs were detected. The X-ray crystal structure of the hCA II adduct with morpholine dithiocarbamate evidenced the inhibition mechanism of these compounds, which coordinate to the metal ion through a sulfur atom from the dithiocarbamate zinc-binding function. Some dithiocarbamates showed an effective intraocular pressure lowering activity in an animal model of glaucoma.



### **I** INTRODUCTION

Carbonic anhydrases (CAs, EC 4.2.1.1) are widespread zinc metalloenzymes found in higher vertebrates including humans.<sup>1–3</sup> Sixteen isozymes have been characterized to date, many of which are involved in critical physiological processes. They catalyze the following reaction:  $\text{CO}_2 + \text{H}_2\text{O} \leftrightarrow \text{H}^+ + \text{HCO}_3^-$ .<sup>1–3</sup> In humans, CAs are present in a large variety of tissues including the gastrointestinal tract, the reproductive tract, the nervous system, kidneys, lungs, skin, and eyes.<sup>2,3</sup> The different isozymes are localized in different parts of the cell with CA I and CA II, important isozymes in normal cells being localized in the cytosol.<sup>1–4</sup>

Many of the CA isozymes are important therapeutic targets with the potential to be inhibited to treat a range of disorders.<sup>1–7</sup> CA II plays a role in bicarbonate production in the eye and is therefore a target for therapy of eye diseases such as glaucoma.<sup>7–9</sup> Indeed, CA inhibitors (CAIs) of the sulfonamide type such as dorzolamide (DZA) or brinzolamide (BRZ) are topically used antiglaucoma agents,<sup>7–10</sup> whereas the older drugs, such as acetazolamide (AAZ) or dichlorophenamide (DCP) show the same action through systemic administration, which, however, leads to a wide range of side effects due to inhibition of the enzyme from other organs than the target one, that is, the eye.<sup>11</sup> CA XII, a transmembrane isoform with an extracellular active site, was shown to be overexpressed in glaucomatous patients eyes.<sup>12</sup>



As some solid tumors grow in cancer patients, hypoxic regions are formed, particularly in the interior of the tumor.<sup>13</sup> The gene expression profile of a hypoxic cancer cell is different from that of other cancer cells in a normally oxygenated environment, that is, in normoxic conditions.<sup>13–15</sup> Under hypoxia, the distribution of CA isoforms is altered as compared with normoxic cells.<sup>13,14</sup> As a result, CA isozymes IX and XII are overexpressed in hypoxic tumor cells, in a variety of solid tumors.<sup>13–15</sup> Unlike other CAs, CA IX and CA XII are both extracellularly localized on hypoxic tumor cells.<sup>13–15</sup> These enzymes play various roles in tumorigenesis, by regulating pH inside and outside the tumor cell,<sup>15</sup> interfering with

Received: November 22, 2011

Published: January 26, 2012

phosphorylation of various proteins,<sup>16</sup> or playing a role in the cell–cell adhesion.<sup>13–15</sup> They therefore provide a target for cancer therapy because they are relatively specific to the hypoxic tumor cells and appear to be important in their survival and proliferation.<sup>15</sup> Indeed, several antibodies targeting CA IX are in phase III clinical development for the treatment of solid tumors (or for their imaging),<sup>17</sup> whereas some small molecule inhibitors are also in advanced preclinical evaluation.<sup>15,18,19</sup>

The classical CAIs are the sulfonamides and their isosteres (sulfamates, sulfamides, etc.).<sup>1–4</sup> However, most of these compounds indiscriminately inhibit many of the 16 CA isoforms known to date in mammals.<sup>1–3</sup> Thus, efforts have been made to find different CAIs, from the sulfonamide, sulfamate, and sulfamide ones. Indeed, recently, the coumarins were discovered as mechanism-based inhibitors that act as prodrugs and bind in a very different mode as compared to sulfonamides and their isosteres,<sup>20</sup> whereas some polyamines (such as spermine),<sup>21</sup> as well as a range of phenols,<sup>22</sup> were also investigated and showed such interesting properties and novel mechanisms of inhibition. Among CAIs investigated to date, there are also the inorganic anions, which coordinate to the zinc ion from the enzyme active site.<sup>1,23,24</sup> Indeed, trithiocarbonate ( $\text{CS}_3^{2-}$ ), an anion similar to carbonate, has recently been investigated and shown to constitute a “lead” for novel CAIs.<sup>23</sup> The X-ray crystal structure for the adduct of trithiocarbonate ( $\text{CS}_3^{2-}$ ), bound to hCA II, has recently been reported (Figure 1).<sup>23</sup> The inhibitor binds to the  $\text{Zn}^{2+}$  in the hCA II active site in

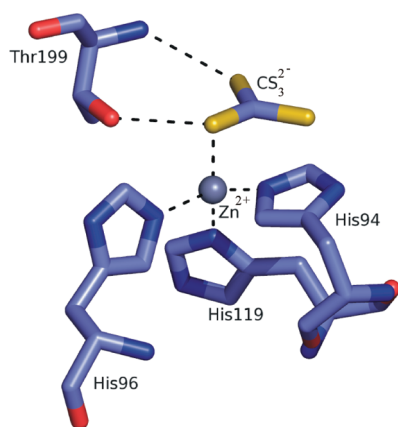


**Figure 1.** Trithiocarbonate ( $\text{CS}_3^{2-}$ ), a recently investigated low micromolar CAI, binds to the  $\text{Zn}^{2+}$  in the hCA II active site in a slightly distorted tetrahedral geometry of the metal ion, occupying a position similar to that observed in the case of the hCA II–bicarbonate complex. The protein zinc ligands (His94, -96, and -119) and Thr199 are shown (PDB code 3K7K).<sup>24</sup>

a slightly distorted tetrahedral geometry of the metal ion, occupying a position similar to that observed in the case of the hCA II–bicarbonate complex.<sup>23</sup> Trithiocarbonate was mono-coordinated to the  $\text{Zn}(\text{II})$  ion by means of one of the sulfur atoms. The same sulfur made a hydrogen bond to the OH of Thr199, whereas a second sulfur atom participated with another hydrogen bond to the NH group of the same amino acid residues, Thr199. This binding mode explains the low micromolar affinity of this inhibitor to many of the CA isoforms investigated to date.<sup>23</sup> On the basis of this binding mode of a millimolar inhibitor, trithiocarbonate ( $\text{CS}_3^{2-}$ ), we hypothesized that compounds incorporating this new zinc-binding function,  $\text{CS}_2^-$ , may act as even stronger CAIs. Indeed, we have recently

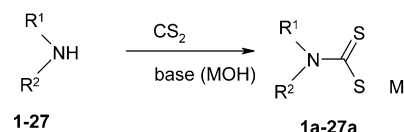
demonstrated in a preliminary communication that dithiocarbamates (DTCs), compounds possessing the general formula  $\text{R}^1\text{R}^2\text{N-CS}_2^-\text{M}^+$ , act as highly efficient CAIs.<sup>25</sup> Here, we report the first detailed study of the DTCs as a class of potent CAIs, with a mechanism of action different of that of the sulfonamides. Furthermore, we prove that some of these highly water-soluble compounds possess excellent intraocular pressure (IOP) lowering properties in an animal model of glaucoma, making them interesting candidates for developing antiglaucoma drugs.

## RESULTS AND DISCUSSION

**Chemistry.** DTCs are well-known metal complexing agents, and they also possess interesting biomedical and agricultural applications.<sup>26–29</sup> Although this class of compounds (and their metal complexes) started to be used as fungicides more than 50 years ago,<sup>29</sup> few studies investigated their interactions with metalloenzymes.<sup>27</sup> Apart from studies of DTCs as inhibitors of tyrosinase, a copper enzyme,<sup>27</sup> only one such work investigated the inhibition of *N,N*-diethyl-DTC with bovine CA (bCA).<sup>28</sup> By using  $\text{Co}(\text{II})$ -substituted CA, Morpurgo et al.<sup>28</sup> showed that the inhibitor does not extrude the metal ion from the enzyme active site (as it does with the copper ion from the tyrosinase active site)<sup>27</sup> and that it binds to it, probably in a trigonal-bipyramidal geometry of  $\text{Co}(\text{II})$ . However, no other DTCs were subsequently investigated for their interaction with CAs until our group reported that trithiocarbonate and related compounds containing the new zinc binding group (ZBG) found in it, that is,  $\text{CS}_2^-$ , inhibit several CA isoforms in the low micromolar or submicromolar range.<sup>23</sup> Here, we extend those findings, showing that a wide range of DTCs incorporating various aliphatic and/or aromatic moieties at the nitrogen atom acts as low nanomolar and even subnanomolar CAIs.

We prepared a series of 27 DTCs, of types **1a–27a**, by the classical reaction<sup>27,30,31</sup> of dithiocarbamylation between primary/secondary amines **1–27** and  $\text{CS}_2$ , in the presence of a base, which most of the time was  $\text{NaOH}$ ,  $\text{KOH}$ , but in the case of more basic amines, the amine itself can act as the base (Scheme 1). As shown in Table 1, a large variety of  $\text{R}^1$  and  $\text{R}^2$

### Scheme 1. Preparation of DTCs **1a–27a** by Reaction of Amines **1–27** with Carbon Disulfide in the Presence of Bases



M = Na, K, alkyl ammonium

moieties are present in DTCs reported here, that is, hydrogen, alkyl, aryl, aralkyl, hetaryl, and cyclic such moieties, which lead to the generation of a wide chemical diversity in these compounds. Presumably, this should be reflected also in varied physicochemical and biological properties of these DTCs. Compounds **1a–27a** were characterized by physicochemical standard procedures (IR,  $^1\text{H}$  and  $^{13}\text{C}$  NMR spectroscopy, MS) and were >99% pure, as determined by HPLC (see the Experimental Protocols for details)

**CA Inhibition.** Compounds **1a–27a** were assayed<sup>32</sup> for the inhibition of four physiologically relevant CA isoforms, hCA I,

Table 1. CA I, II, IX, and XII Inhibition Data with DTCs 1a–27a by a Stopped-Flow, CO<sub>2</sub> Hydrase Assay<sup>32</sup>

no. <sup>a,b</sup>	R <sup>1</sup>	R <sup>2</sup>	R <sup>1</sup> R <sup>2</sup> N-CSS <sup>-</sup> M <sup>+</sup>			
			1a–27a			
			K <sub>i</sub> (nM) <sup>c</sup>			
			hCA I	hCA II	hCA IX	hCA XII
1a	H	Ph	4.8	4.5	4.2	4.3
2a	H	O[(CH <sub>2</sub> CH <sub>2</sub> ) <sub>2</sub> N	4.8	3.6	29.1	9.2
3a	H	MeN[(CH <sub>2</sub> CH <sub>2</sub> ) <sub>2</sub> N	33.5	33.0	22.1	17.5
4a	H	2-butyl	21.1	29.4	4.6	31.7
5a	H	O[(CH <sub>2</sub> CH <sub>2</sub> ) <sub>2</sub> N(CH <sub>2</sub> ) <sub>2</sub>	31.8	36.3	4.5	4.2
6a	H	N[(CH <sub>2</sub> CH <sub>2</sub> ) <sub>2</sub> N] <sub>3</sub>	31.9	13.5	27.4	9.3
7a	H	PhCH <sub>2</sub>	4.1	0.70	19.2	11.5
8a	H	4-pyridylCH <sub>2</sub>	3.5	16.6	26.0	24.1
9a	H	[(CH <sub>2</sub> ) <sub>5</sub> N]CH <sub>2</sub> CH <sub>2</sub>	4.5	20.3	3.6	20.5
10a	H	2-thiazolyl	3.9	4.6	12.6	22.0
11a	H	KOOCCH <sub>2</sub>	13.1	325	57.1	6.7
12a	H	imidazol-1-yl-(CH <sub>2</sub> ) <sub>3</sub>	8.6	24.7	4.3	6.5
13a	Me	Me	699	6910	714	798
14a	Et	Et	790	3100	1413	1105
15a	(CH <sub>2</sub> ) <sub>5</sub>		0.96	27.5	70.4	46.1
16a	<i>iso</i> -Bu	<i>iso</i> -Bu	0.97	0.95	4.5	0.99
17a	<i>n</i> -Pr	<i>n</i> -Pr	1838	55.5	53.8	7.0
18a	<i>n</i> -Bu	<i>n</i> -Bu	43.1	50.9	50.3	5.8
19a	<i>n</i> -Hex	<i>n</i> -Hex	48.0	51.3	27.4	16.1
20a	Et	<i>n</i> -Bu	157	27.8	25.9	7.5
21a	HOCH <sub>2</sub> CH <sub>2</sub>	HOCH <sub>2</sub> CH <sub>2</sub>	9.2	4.0	4.3	4.2
22a	Me	Ph	39.6	21.5	28.2	7.7
23a	Me	PhCH <sub>2</sub>	69.9	25.4	53.0	3.0
24a	O[(CH <sub>2</sub> CH <sub>2</sub> ) <sub>2</sub>		0.88	0.95	6.2	3.4
25a	NaS(S=C)N[(CH <sub>2</sub> CH <sub>2</sub> ) <sub>2</sub>		12.6	0.92	37.5	0.78
26a	(NC)(Ph)C(CH <sub>2</sub> CH <sub>2</sub> ) <sub>2</sub>		48.4	40.8	757	169
27a	( <i>S</i> )-[CH <sub>2</sub> CH <sub>2</sub> CH <sub>2</sub> CH(COONa)]		2.5	17.3	4.1	4.0
AAZ			250	12	25	5.7

<sup>a</sup>Compounds 1a, 8a, and 10a were triethylammonium salts; 2a–6a, 9a, 11a, and 12a were potassium salts, and the remaining ones were sodium salts.

<sup>b</sup>Means from three different assays. Errors were within  $\pm 5$ –10% of the reported values (data not shown). <sup>c</sup>Inhibition data against hCA I, II, and IX for nine DTCs; that is, compounds 13a, 14a, 16–18a, 20a, 22a, 23a, and 26a were reported in ref 25.

II, IX, and XII. All of them are drug targets: hCA I, II, and XII for ophthalmologic diseases, mainly glaucoma,<sup>1,10</sup> whereas CA IX and XII for antitumor drugs/tumor imaging agents.<sup>1,15,17–19</sup> Inhibition data with the sulfonamide, clinically used agent AAZ are also reported in Table 1, for comparison reasons.

The following structure–activity relationship (SAR) can be observed for the CA inhibition data with DTCs 1a–27a investigated here:

- The cytosolic isoform hCA I was strongly inhibited by DTCs 1a–27a investigated here, with  $K_i$  values in the range of 0.88–1838 nM. It may be observed that irrespective of the nature of R<sup>2</sup>, the DTCs prepared from primary amines (R<sup>1</sup> = H) 1a–12a were highly effective hCA I inhibitors, with inhibition constants in the low nanomolar range (3.5–33.5 nM). On the contrary, the compounds prepared from secondary amines showed a more varied biological activity. Thus, the simple dimethyl- and diethyl-DTCs 13a and 14a were weak hCA I inhibitors, with  $K_i$  values in the range of 699–790 nM. The same is true for the di-*n*-propyl derivative 17a ( $K_i$  of 1838 nM). However, the cyclic derivative 15a, which differs from 14a by the cyclic structure and an extra carbon atom present in its molecule, is a subnanomolar hCA I inhibitor, showing a dramatic

increase of potency of 823 times as compared to 14a. It is also interesting to compare the potencies of 16a and 18a, which incorporate *iso*-butyl and *n*-butyl moieties (and are isomers) and differ by a factor of 44, unexpectedly, in favor of the compound with a branched scaffold. Increasing the length of the aliphatic chains to C6, as in 19a, leads to a slight loss of potency as compared to the most active compounds in the aliphatic series, which are 15a and 16a. Furthermore, the presence of hydroxyethyl moieties (instead of the ethyl ones) as in 21a leads to a steady increase of potency, 21a being 85.9 times a better hCA I inhibitor as compared to 14a. The compounds incorporating one alkyl and one aryl moiety at the nitrogen atom of the DTC function, such as 22a and 23a, were also effective hCA I inhibitors ( $K_i$  values of 39.6–69.9 nM), as were also the heterocyclic derivatives 24a–27a, some of which showed subnanomolar activity (the morpholine DTC 24a had a  $K_i$  of 0.88 nM and was the best DTC hCA I inhibitor and also the best hCA I inhibitor ever described, as far as we know). Thus, many of these chemotypes explored here show excellent hCA I inhibitory activity, which range from the subnanomolar to the micromolar. Furthermore, many of the DTCs are much more effective as hCA I inhibitors as

compared to the sulfonamide AAZ, which has a  $K_i$  of 250 nM against this isoform (Table 1).

- (ii) The physiologically dominant cytosolic isoform hCA II also showed an interesting inhibition profile with DTCs **1a–27a**. Thus, several primary DTCs (**1a**, **2a**, **7a**, and **10a**) and several secondary ones (**16a**, **21a**, **24a**, and **25a**) were excellent hCA II inhibitors, with  $K_i$  values in the range of 0.70–4.6 nM, being more effective (even 1 order of magnitude) than the clinically used sulfonamide AAZ (Table 1). It may be observed that these compounds incorporate aromatic, arylalkyl, hetaryl, alkyl, and hydroxyalkyl moieties substituting the nitrogen atom from the DTC moiety. Another rather large group of derivatives, such as **3a–6a**, **8a**, **9a**, **12a**, **15a**, **17a–20a**, **22a**, **23a**, **26a**, and **27a**, were slightly less effective hCA II inhibitors but still possessed a high efficacy, with  $K_i$  values in the range of 13.5–55.5 nM. Again, both primary and secondary DTCs are present in this subgroup. They incorporate various types of substituents, such as alkyl, aryl, aralkyl, and hetaryl ones. It is obvious that small structural changes in the DTC scaffold influence dramatically the biological activity. For example, for the aliphatic secondary DTCs, the isomeric pair **16a–18a**, which differ only by the nature of the aliphatic chain (*iso*-Bu moieties in the first compound and *n*-Bu in the second derivative), have  $K_i$  values that differ by a factor of 53.6. The length of the alkyl chain also strongly influence activity, with compounds possessing a medium chain (e.g., **15a–20a**) being more effective than the ones with shorter chains, such as **13a** and **14a**, which are rather ineffective as hCA II inhibitors ( $K_i$  values of 3.1–6.9  $\mu$ M). Also, the glycine DTC **11a** was a medium potency hCA II inhibitor, with a  $K_i$  of 325 nM.
- (iii) The tumor-associated isoform hCA IX was highly inhibited by the DTCs investigated here, with  $K_i$  values in the range of 3.6–1413 nM. The simple aliphatic secondary DTCs **13a/14a** and the bulky cyclic derivative **26a** were the least effective inhibitors ( $K_i$  values of 0.714–1.413  $\mu$ M), and four other compounds (**11a**, **15a**, **17a**, and **18a**) were effective, medium potency inhibitors, with  $K_i$  values in the range of 50.3–70.4 nM. They incorporate the carboxyalkyl moiety present in glycine (**11a**), the five-membered aliphatic ring (from **15a**), and 3- or 4-carbon atom *n*-alkyl chains (**17a** and **18a**). All of the remaining derivatives showed highly effective hCA IX inhibitory properties, with  $K_i$  values < 30 nM. Thus, a rather high structural diversity (aliphatic, aromatic, aralkyl, hetaryl moieties) present in primary/secondary DTCs lead to highly effective hCA IX inhibitors, with minor structural changes drastically affecting enzyme inhibition. Many DTCs were more effective hCA IX inhibitors as compared to AAZ (Table 1).
- (iv) A rather similar SAR as the one discussed above for hCA IX was observed for the inhibition of the second transmembrane isoform, hCA XII, with DTCs **1a–27a**. Thus, **13a/14a** and **26a** were the least effective inhibitors ( $K_i$  values in the range of 169–1105 nM), whereas the remaining DTCs were highly effective hCA XII inhibitors, with  $K_i$  values in the range of 0.78–31.7 nM (Table 1). Among the best hCA XII inhibitors (subnanomolar inhibition constants) were the diisobutyl-DTC **16a** and the piperazine-bis-DTC **25a**.

Again, the main conclusion is that a large number of substitution patterns, incorporating varied moieties, lead to highly effective hCA XII inhibitors.

- (v) The DTCs investigated here showed a rather promiscuous inhibitory activity against all four CA isoforms described here, although each of these CAs had a different inhibition profile with all of these compounds. For example, **15a** was a subnanomolar inhibitor of hCA I and inhibited the remaining three isoforms with  $K_i$  values in the range of 27.5–70.4 nM, having thus an acceptable selectivity ratio for the inhibition of hCA I over the remaining three CAs. Compound **25a** was a subnanomolar inhibitor of hCA II and XII and inhibited hCA I and IX with higher  $K_i$  values, of 12.6–37.5 nM. Compound **23a** showed a rather good selectivity for inhibiting hCA XII over hCA I, II, and IX (Table 1). It should be also mentioned that being negatively charged, these compounds show membrane impermeability,<sup>33</sup> which may be a favorable pharmacological property in vivo.

**X-ray Crystallography.** To explain the potent CA inhibitory properties of the DTCs, which are a new class of CAIs, we resolved the X-ray crystal structure of hCA II in complex with the very potent inhibitor **24a** ( $K_i$  of 0.95 nM). Compound **24a** was well ordered and refined with an occupancy of 1.0 with *B* factors that were comparable to the solvent within the active site (Table 2). The compound is

**Table 2. Crystallographic Data Refinement and Model Quality Statistics for the hCA II–24a Complex<sup>a</sup>**

PDB accession number	3PSA
data collection statistics	
temperature (K)	100
wavelength (Å)	1.5418
space group	<i>P</i> 2 <sub>1</sub>
unit cell parameters (Å, °)	<i>a</i> = 42.3; <i>b</i> = 41.2 <i>c</i> = 72.1; $\beta$ = 104.2
total theoretical reflections	39632
total measured reflections	39395
resolution (Å)	50.0–1.5 (1.54–1.50)
$R_{\text{sym}}$ (%); <i>I</i> / $\sigma$ ( <i>I</i> ) <sup>b</sup>	6.4 (18.1); 17.5 (5.8)
completeness; redundancy	99.4 (95.7); 3.7 (3.4)
final model statistics	
$R_{\text{cryst}}$ (%); <sup>c</sup> $R_{\text{free}}$ (%) <sup>d</sup>	0.148; 0.169
residue nos.	4–261
no. of protein atoms <sup>e</sup>	2078
no. of compound atoms	9
no. of H <sub>2</sub> O molecules	300
RMSD bond lengths (Å)	0.012
RMSD bond angles (°)	1.488
Ramachandran statistics (%)	89.4, 10.7, 0.0
average <i>B</i> factors (Å <sup>2</sup> ) main, side chain, compound, solvent	13.6, 18.1, 23.9, 29.4

<sup>a</sup>Values in parentheses represent the highest resolution bin. <sup>b</sup> $R_{\text{sym}} = \sum |I - \langle I \rangle| / \sum \langle I \rangle$ . <sup>c</sup> $R_{\text{cryst}} = (\sum |F_o| - |F_c|) / \sum |F_o| \times 100$ . <sup>d</sup> $R_{\text{free}}$  is calculated in same manner as  $R_{\text{cryst}}$  except that it uses 5% of the reflection data omitted from refinement. <sup>e</sup>Includes alternate conformations.

buried deep into the active site, displacing the catalytic zinc-bound solvent, such that one of the sulfur atoms coordinates directly to the zinc ion of the enzyme. The overall zinc coordination (3N from the coordinating histidine residues



His94, -96, and -119 and 1S from the inhibitor ligand) can be described as a distorted tetrahedron (Figure 2). The details of

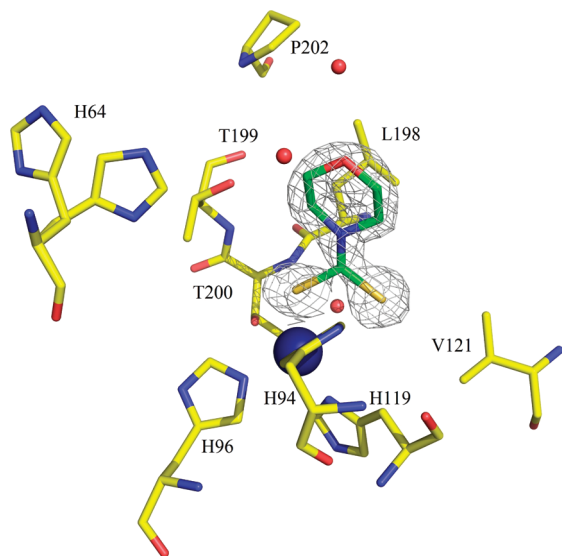


**Figure 2.** Stick representation of the hCA II active site with compound **24a** (green) complexed within it. The active-site zinc is depicted as a blue sphere. Water molecules are depicted as red spheres. The electron density is represented by a  $\sigma$ -weighted  $2F_o - F_c$  Fourier map (gray mesh). Amino acids involved in the binding of inhibitor are also shown. The figure was made using PyMOL (DeLano Scientific).

**Table 3. Geometry of the Zn(II) Ion and Bound S Atom (of the DTCs) for Compounds 23a, 24a, and 26a Complexed within the hCA II Active Site (Angle Defined as His–Zn–S)**

	23a	24a	26a
distance (Å)	2.3	2.3	2.3
angle (deg) with His94	111.3	107.3	108.8
angle (deg) with His96	114.2	112.2	112.9
angle (deg) with His119	119.4	128.3	126.1

this tetrahedral geometry are provided in Table 3. The zinc-bound sulfur also interacts with the O atom of Thr199 in a similar manner to that observed in the more classical clinically used sulfonamides and sulfamates CAIs.<sup>34–36</sup> Compound **24a** possesses a puckered ring and binds with a slightly higher *B* factor of 23.9 Å<sup>2</sup>, as compared to the two other DTCs for which the X-ray structure in complex with hCA II was reported earlier,<sup>25</sup> that is, **23a** and **26a**. For a structural comparison, the three compounds were superposed onto each other (Figure 3). For unbound hCA II, the side chain conformation of His64 has been shown to be dependent upon the buffer pH, which affects the protonation state of the imidazole ring. It is widely believed that this side chain flips from an “in” to “out” conformation as part of the proton transfer mechanism in hCA II; hence, two conformations of the residue are often observed in crystal structures.<sup>34–36</sup> His64 in the hCA II structure in complex with compounds **26a** (PDB ID: 3P5L) and **24a** (PDB ID: 3P5A) has a dual conformation. In the case of **26a**, the terminal six-membered hydrophobic ring sits close to F131, V135, and P202 at the rim of the active site in a hydrophobic pocket of hCA II. Whereas for **24a**, the six-membered ring does not extend far enough out of the active site to either reach this hydrophobic pocket or close enough to the in-conformation of His64. Hence, compounds **24a** and **26a** are 5.6 and 5.0 Å, respectively, from His64 and therefore do not affect its conformation. Whereas in the hCA II–**23a** structure (PDB ID: 3P58), the six-membered planar ring forms a T-shaped  $\pi$ -stacking with the imidazole ring of His64 and stabilizes this amino acid in the “in” conformation.<sup>25</sup> In addition, **24a** is positioned 3.2 Å from Thr200 but does not form hydrogen bonds with either the protein main or the side chain. However, the endocyclic oxygen atom in the tail ring of **24a** was within hydrogen bond distance of 3.4 and 3.2 Å from water393 and water540, respectively (Figure 2), which probably also contributes to its high affinity to hCA II.

**Intraocular Pressure Lowering in Hypertensive Rabbits.** Two of the new CAIs investigated here, compounds **24a** and **25a**, which show excellent hCA II and XII inhibitory properties (Table 1), were investigated in vivo, for their ability to lower IOP in carbomer-induced glaucoma in rabbits.<sup>10c</sup> Normal IOP in rabbits, like in humans, is around 15–20

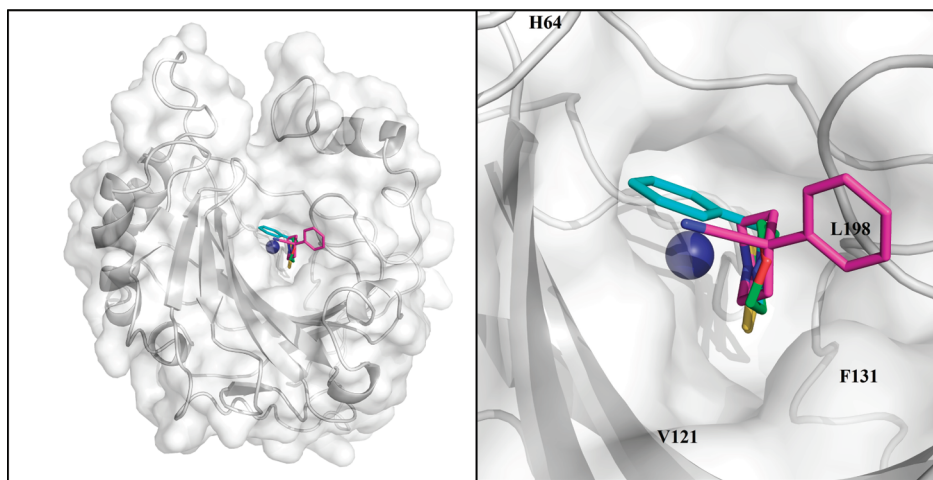


**Figure 3.** View of compounds **23a** (cyan), **24a** (green), and **26a** (magenta) superposed in the active site of hCA II. The left and right panel depict overall and zoomed active-site views, respectively. hCA II is depicted as a gray surface representation. The active-site zinc is depicted as a blue sphere. The figure was made using PyMOL (DeLano Scientific).

mmHg. In this model, the IOP is quite elevated, thus mimicking the pathologic situation observed in the human disease.<sup>10</sup> Clinically used drugs such as DZA induce a maximal IOP lowering of 4–5 mmHg, as reported recently by us.<sup>10</sup> The two DTCs investigated here in detail were chosen both due to their excellent enzyme inhibitory activity in vitro and also because they show very good water solubility, being formulated at 2% eye drop solution at neutral pH (due to their salt character, whereas DZA is formulated at pH 5.5, as a hydrochloride salt, and induces eye irritation).<sup>10</sup> In fact, water solubility of eye drugs is a significant problem,<sup>8–10</sup> with many classes of drugs achieving an acceptable solubility only as salts with strong acids, such as HCl, which leads to acidic pH values causing eye irritation (DZA is a well-known case).<sup>10</sup>

Rabbits were treated with 2% solutions of DTCs **24a** and **25a**, and their IOP was monitored for 48 h (Figure 4a). The

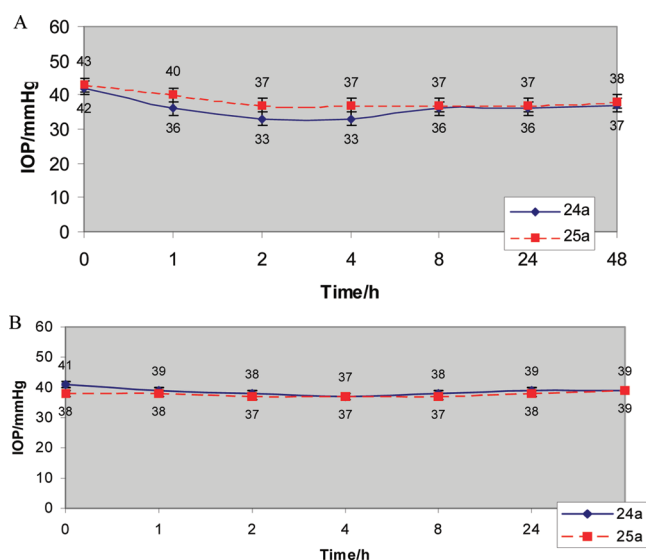


**Figure 4.** (A) IOP lowering vs time of glaucomatous rabbits treated with one drop (50  $\mu$ L) of a 2% water solution of DTC **24a** and **25a**. (B) IOP in the eyes treated with vehicle (IOP are the means from three different animals). Error bars are shown in both figures, accounting for an average of 0.8–1.5 mmHg.

contralateral eye was treated with vehicle and was used as control (Figure 4B). As observed from Figure 4, both compounds were effective in reducing elevated IOP time dependently for a rather long period. The maximal effect (of –6–10 mmHg) has been observed after 2 h postadministration, and it lasted for up to 4–8 h, being almost double that reported for DZA (of 4–5 mmHg and lasting only for about 3–4 h).<sup>10</sup> DTC **24a** was slightly more effective than **25a** as an IOP lowering agent. The IOP in vehicle-treated eyes was rather constant during the entire duration of the experiments, varying between 37 and 39 mmHg for animals treated with **25a** and between 37 and 40 mmHg for animals treated with **24a** (the data of the figures are the mean for three different animals, and the error range is shown in Figure 4).

## CONCLUSIONS

We report here that DTCs represent a novel class of highly effective CAIs. DTCs are easy to prepare from simple starting materials, they can incorporate a very high chemical diversity, and they act as inhibitors of several physiologically relevant CA isoforms, with potencies from the subnanomolar to the

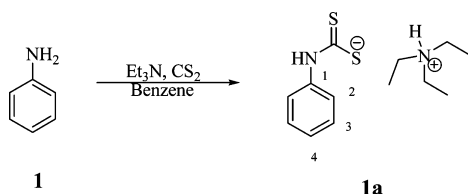
micromolar. SARs for the inhibition of isoforms hCA I, II, IX, and XII were straightforward and slightly different, with small modifications in the backbone of the compound leading to dramatic changes of biological activity. The inhibition mechanism of the DTCs was also explained, by resolving the X-ray crystal structure for hCA II complexed with a heterocyclic DTC. The  $\text{CS}_2^-$  moiety present in DTCs represents a new zinc-binding function. It is directly coordinated to the Zn(II) ion from the enzyme active site and also participates in an interaction (hydrogen bond) with the OH moiety of Thr199, an amino acid essential for the binding of many classes of CAIs (and of the substrates). The organic scaffold of the DTC is deeply buried within the enzyme active site and also participates in favorable interactions with it, which leads to a high stabilization of the enzyme–inhibitor adduct. Some of the most potent CAIs detected here showed favorable IOP lowering effects in an animal model of glaucoma. Being water-soluble, with the pH of the solution in the neutral range and with duration of action lasting up to 4–8 h, this new class of CAIs may constitute interesting candidates for developing novel antiglaucoma therapies, a field in which no new drug has emerged in the last 15 years.

## EXPERIMENTAL PROTOCOLS

**Chemistry.**  $^1\text{H}$ ,  $^{13}\text{C}$ , DEPT, COSY, HMQC, and HMBC spectra were recorded using a Bruker Advance III 400 MHz spectrometer. The chemical shifts are reported in parts per million (ppm), and the coupling constants ( $J$ ) are expressed in Hertz (Hz). For all new compounds, DEPT, COSY, HMQC, and HMBC were routinely used to definitely assign the signals of  $^1\text{H}$  and  $^{13}\text{C}$ . Infrared spectra were recorded on a Perkin-Elmer Spectrum R XI spectrometer as solids on KBr plates. Melting points (mp) were measured in open capillary tubes, unless otherwise stated, using a Büchi Melting Point B-540 melting point apparatus and are uncorrected. Thin-layer chromatography (TLC) was carried out on Merck silica gel 60  $F_{254}$  aluminum-backed plates. Elution of the plates was carried out using ethyl acetate/*n*-hexane or MeOH/DCM systems. Visualization was achieved with UV light at 254 nm, by dipping into a 0.5% aqueous potassium permanganate solution, by Hanessian's stain solution, and heating with a hot air gun or by exposure to iodine.

All other solvents and chemicals were used as supplied from Aldrich Chemical Co., Acros, Fisher, Alfa Aesar, or Lancaster Synthesis. Aniline **1**, morpholin-4-amine **2**, 4-methylpiperazin-1-amine **3**, ( $\pm$ ) *sec*-butylamine **4**, 2-morpholinoethanamine **5**,  $N_1, N_1$ -bis(2-aminoethyl)ethane-1,2-diamine **6** (Tris), benzylamine **7** (CAS 100-46-9), pyridin-4-ylmethanamine **8** (CAS 3731-53-1), 2'-(piperidin-1-yl)ethanamine **9**, 2-aminothiazole **10**, glycine **11**, 3-(1*H*-imidazol-1-yl)propan-1-amine **12**, sodium dimethyldithiocarbamate **13a**, sodium diethyldithiocarbamate **14a**, pyrrolidine **15**, diisobutylamine **16**, dipropylamine **17**, dibutylamine **18**, dihexylamine **19**, ethylbutylamine **20**, diethanolamine **21**, *N*-methylbenzenamine **22**, *N,N*-benzylmethylamine **23**, morpholine **24**, piperazine **25**, 4-cyano-4-phenylpiperidine hydrochloride **26**, and *L*-proline **27** were purchased from Sigma-Aldrich (Milan, Italy) and were of the highest available purity. The purity of the prepared DTCs has been determined by HPLC and was >99%.

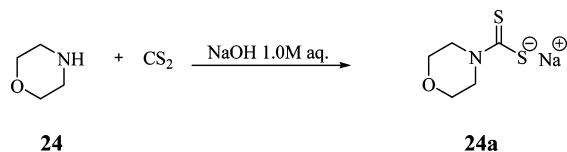
**General Procedure for the Synthesis of Compounds 1a–27a.**<sup>30</sup> Secondary/primary amines **1–27** (1.0 g, 1.0 equiv) were treated with a NaOH, KOH, or  $\text{Et}_3\text{N}$  (1.0–2.2 equiv), 4.0 mL of MeOH as a cosolvent was used, and the solutions were stirred at 0  $^\circ\text{C}$  for 20 min (Scheme 1). Then, carbon disulfide (1.2–2.4 equiv) was added dropwise, and the mixture was stirred at r.t. until starting material was consumed (TLC monitoring). The solvents were removed under vacuo at r.t., and the residues obtained were dissolved in MeOH and filtered off through Celite, and the filtrate was concentrated in vacuo not exceeding 20  $^\circ\text{C}$ .

Synthesis of Triethylammonium Phenylcarbamodithioate **1a**.

Aniline **1** (0.5 g, 1.0 equiv) was treated with triethylamine (1.0 equiv) in benzene (0.5 mL) followed by the addition of carbon disulfide (1.0 equiv) at 0 °C. The mixture was warmed to r.t. and stirred O.N. at r.t. The solid formed was washed with diethyl ether and dried under vacuo to afford the titled compound as a light yellow solid in 51% yield.

**Triethylammonium Phenylcarbamodithioate 1a.**  $\nu_{\max}$  (KBr)  $\text{cm}^{-1}$ : 2960, 2886, 1648, 1599, 1520, 1451.  $\delta_{\text{H}}$  (400 MHz, DMSO- $d_6$ ): 1.13 (9H, t,  $J = 6.8$ ,  $3 \times \text{CH}_2\text{CH}_3$ ), 2.98 (6H, brs,  $3 \times \text{CH}_2\text{CH}_3$ ), 6.97 (1H, t,  $J = 8.0$ , 4-H), 7.22 (2H, dd,  $J = 8.3$ , 8.0, 2  $\times$  3-H), 7.93 (2H, d,  $J = 8.3$ , 2  $\times$  2-H), 9.00 (1H, brs, exchange with  $\text{D}_2\text{O}$ ,  $(\text{CH}_3\text{CH}_2)_3\text{N}^+\text{-H}$ ), 10.10 (1H, brs, exchange with  $\text{D}_2\text{O}$ , N-H).  $\delta_{\text{C}}$  (100 MHz, DMSO- $d_6$ ): 10.0, 46.6, 114.8, 122.9, 128.4, 143.2, 215.5 (C=S).  $m/z$  (ESI), 168  $[\text{M} - \text{Na}]^-$ .

**Diisobutylcarbodithioic Acid Sodium Salt 16a.** mp 220 °C with dec.  $\nu_{\max}$  (KBr)  $\text{cm}^{-1}$ : 2961, 2933, 2867, 1640, 1601, 1520, 1480, 1090.  $\delta_{\text{H}}$  (400 MHz, DMSO- $d_6$ ): 0.84 (12H, d,  $J = 6.8$ ,  $4 \times \text{CH}_3$ ), 2.43 (4H, m, 2  $\times$  CH), 3.86 (4H, d,  $J = 7.2$ , 2  $\times$   $\text{CH}_2$ ).  $\delta_{\text{C}}$  (100 MHz, DMSO- $d_6$ ): 21.2, 27.4, 61.5, 215.4 (C=S).  $m/z$  (ESI), 204  $[\text{M} - \text{Na}]^-$ . Data are in agreement with reported data.<sup>30</sup>

Synthesis of Morpholinecarbamodithioate Sodium Salt **24a**.

Morpholine **24** (1.0 g, 1.0 equiv) was treated according to the general procedure with 1.0 M aqueous solution of NaOH (1.0 equiv) followed by the addition of carbon disulfide (1.2 equiv). The title compound was obtained as a white solid in quantitative yield.

**Morpholinecarbamodithioate Sodium Salt 24a.** mp 320 °C with dec.  $\nu_{\max}$  (KBr)  $\text{cm}^{-1}$ : 2966, 2901, 2854, 1625, 1520, 1416, 1215.  $\delta_{\text{H}}$  (400 MHz, DMSO- $d_6$ ): 3.52 (4H, t,  $J = 8.0$   $\text{CH}_2$ ), 4.33 (2H, t,  $J = 8.0$ ,  $\text{CH}_2$ ).  $\delta_{\text{C}}$  (100 MHz, DMSO- $d_6$ ): 50.6, 67.1, 215.4 (C=S).  $m/z$  (ESI), 162  $[\text{M} - \text{Na}]^-$ .

**CA Inhibition.** An Applied Photophysics stopped-flow instrument has been used for assaying the CA-catalyzed  $\text{CO}_2$  hydration activity. Phenol red (at a concentration of 0.2 mM) has been used as an indicator, working at the absorbance maximum of 557 nm, with 20 mM Hepes (pH 7.5) as the buffer, and 20 mM  $\text{Na}_2\text{SO}_4$  (for maintaining constant the ionic strength), following the initial rates of the CA-catalyzed  $\text{CO}_2$  hydration reaction for a period of 10–100 s.<sup>32</sup> The  $\text{CO}_2$  concentrations ranged from 1.7 to 17 mM for the determination of the kinetic parameters and inhibition constants. For each inhibitor, at least six traces of the initial 5–10% of the reaction have been used for determining the initial velocity. The uncatalyzed rates were determined in the same manner and subtracted from the total observed rates. Stock solutions of inhibitor (0.1 mM) were prepared in distilled–deionized water, and dilutions up to 0.01 nM were done thereafter with distilled–deionized water. Inhibitor and enzyme solutions were preincubated together for 15 min at room temperature prior to assay, to allow for the formation of the E–I complex. The inhibition constants were obtained by nonlinear least-squares methods using PRISM 3, as reported earlier,<sup>33</sup> and represent the mean from at least three different determinations. All CA isofoms were recombinant ones obtained in house as reported earlier.<sup>9,10</sup>

**Cocrystallization and X-ray Data Collection of CA II Complex.** Cocrystals for the hCA II–**24a** complex were obtained using the hanging drop vapor diffusion method.<sup>37</sup> Drops of 10  $\mu\text{L}$  (0.3 mM hCA II, 0.7 mM DTC **24a**, 0.1% dimethyl sulfoxide, 0.8 M sodium citrate, and 50 mM Tris-HCl; pH 8.0) were equilibrated against the precipitant solution (1.6 M sodium citrate and 50 mM Tris-HCl; pH 8.0) at room temperature ( $\sim 20$  °C). Crystals were observed after 5 days. On the basis of visual selection, a crystal of the complex was cryoprotected by quick immersion into 20% glycerol precipitant solution and flash-cooled by exposing to a gaseous stream of nitrogen at 100 K. The X-ray diffraction data were collected using an R-AXIS IV<sup>+</sup> image plate system on a Rigaku RU-H3R Cu rotating anode operating at 50 kV and 22 mA, using Osmic Varimax HR optics. The detector–crystal distance was set to 80 mm. The oscillation steps were 1° with a 5 min exposure per image. Indexing, integration, and scaling were performed using HKL2000.<sup>38</sup>

**Structure Determination of CA II Drug Complex.** Starting phases were calculated from Protein Data Bank (PDB) entry 3KS3<sup>39</sup> with waters removed. Refinement using the *Phenix* package,<sup>40</sup> with 5% of the unique reflections selected randomly and excluded from the refinement data set for the purpose of  $R_{\text{free}}$  calculations,<sup>41</sup> was alternated with manual refitting of the model in *Coot*.<sup>42</sup> The validity of the final model was assessed by *PROCHECK*.<sup>43</sup> Complete refinement statistics and model quality are included in Table 2.

**Animals and Glaucoma Induction.** Adult male New Zealand Albino rabbits weighing 2–2.5 kg were employed in this study. The rabbits were utilized in groups of eight for each of the chosen specific treatments. The experimental procedures conformed to those of the Declaration of Helsinki and with the Guideline for the Care and Use of Laboratory Animals as adopted and promulgated by the U.S. National Institute of Health and were conducted upon authorization of the Italian Regulations on Protection of Animals used for experimental and other scientific purpose (DM 116/1992) as well as with the European Union Regulations (OJ of ECL 358/1, 12/12/1986), and the experimental protocol was approved by the local animal care committee of the University of Florence (Florence, Italy). The rabbits were kept in individual cages; food and water were provided ad libitum. The animals were identified with a tattoo on the ear, numbered consecutively, and maintained on a 12–12 h light/dark cycle in a temperature-controlled room (22–23 °C). All selected animals were examined before the beginning of the study and were determined to be normal on ophthalmic and general examinations. Glaucoma was induced by injection of 0.1 mL of 0.25% carbomer (Siccafluid, FarMila—THEA Pharmaceuticals) into anterior eye chamber bilaterally in New Zealand albino rabbits) anesthetized with tiletamine and zolazepam (Zoletil 100, 0.05 mg/kg b.w.) plus xilazine (Xilor 2%, 0.05 mL/kg b.w.) i.m., by the procedure previously reported.<sup>10c</sup> IOP was measured before carbomer injection and after 1, 2, and 4 h the first day and three times a day until stabilization and then every 24 h. All rabbits treated with carbomer presented a net increase in IOP. One drop of 0.2% oxybuprocaine hydrochloride (Novesine, Sandoz) diluted 1:1 with sterile saline was instilled in each eye immediately before each set of pressure measurements. IOP was measured using a Tono-Pen XL tonometer (Medtronic Solan, United States) as reported by earlier.<sup>10</sup> The pressure readings were matched with two-point standard pressure measurements at 1, 2, 4, and 8 h after the instillation of the drug and once a day for the following days using a Digilab calibration verifier. All IOP measurements were done by the same investigators using the same tonometer. As soon as a stable IOP increase was obtained, the animals were treated with the drugs in study. The efficacy of the different drugs in lowering IOP was evaluated after drug administration over 4 hours, with the following schedule: before and after 30, 60, 90, 120, and 240 min after drug administration. The treatment was performed in three animals per drug in one eye and compared to the contralateral eye treated with vehicle. A group of four nonglaucomatous albino rabbits was treated with the drugs of this study and used as control. At the end of the experiments, the animals were killed with a lethal dose of Pentothal (Abbott S.p.A., Campoverde di Aprilia, LT).



## ■ ASSOCIATED CONTENT

### ■ Supporting Information

Complete characterization of compounds 1a–27a. This material is available free of charge via the Internet at <http://pubs.acs.org>.

### Accession Codes

The atomic coordinates of the hCA II-dithiocarbamate adduct (code 3PSA) have been deposited in the Protein Data Base.

## ■ AUTHOR INFORMATION

### Corresponding Author

\*Tel: +39-055-457 3005. Fax: +39-055-4573385. E-mail: [claudiu.supuran@unifi.it](mailto:claudiu.supuran@unifi.it).

### Notes

The authors declare no competing financial interest.

## ■ ACKNOWLEDGMENTS

This research was financed by an FP7 EU project (Metoxia) and a grant from the NIH GM 25154. We thank Dr. G. Formicola and Dr. T. Somma for their collaboration in intraocular pressure measurements.

## ■ ABBREVIATIONS USED

CA, carbonic anhydrase; CAI, carbonic anhydrase inhibitor; DTC, dithiocarbamate

## ■ REFERENCES

- (1) (a) Krishnamurthy, V. M.; Kaufman, G. K.; Urbach, A. R.; Gitlin, I.; Gudiksen, K. L.; Weibel, D. B.; Whitesides, G. M. Carbonic Anhydrase as a Model for Biophysical and Physical-Organic Studies of Proteins and Protein-Ligand Binding. *Chem. Rev.* **2008**, *108*, 946–1051. (b) Zatovicova, M.; Jelenska, L.; Hulikova, A.; Csaderova, L.; Ditte, Z.; Ditte, P.; Goliasova, T.; Pastorek, J.; Pastorekova, S. Carbonic anhydrase IX as an anticancer therapy target: Preclinical evaluation of internalizing monoclonal antibody directed to catalytic domain. *Curr. Pharm. Des.* **2010**, *16*, 3255–3263. (c) Supuran, C. T. Carbonic anhydrases: Novel therapeutic applications for inhibitors and activators. *Nat. Rev. Drug Discovery* **2008**, *7*, 168–181. (d) Supuran, C. T.; Scozzafava, A.; Casini, A. Development of sulfonamide carbonic anhydrase inhibitors (CAIs). In *Carbonic Anhydrase—Its Inhibitors and Activators*; Supuran, C. T., Scozzafava, A., Conway, J., Eds.; CRC Press: Boca Raton, FL, 2004; pp 67–147.
- (2) (a) Supuran, C. T.; Scozzafava, A.; Casini, A. Carbonic anhydrase inhibitors. *Med. Res. Rev.* **2003**, *23*, 146. (b) Pastorekova, P. S.; Pastorek, J.; Supuran, C. T. Carbonic anhydrases: Current state of the art, therapeutic applications and future prospects. *J. Enzyme Inhib. Med. Chem.* **2004**, *19*, 199–229. (c) Thiry, A.; Dogné, J.-M.; Masereel, B.; Supuran, C. T. Targeting tumor-associated carbonic anhydrase IX in cancer therapy. *Trends Pharmacol. Sci.* **2006**, *27*, 566–573.
- (3) (a) Supuran, C. T. Carbonic anhydrase inhibitors. *Bioorg. Med. Chem. Lett.* **2010**, *20*, 3467–3474. (b) Supuran, C. T. Carbonic anhydrase inhibitors and activators for novel therapeutic applications. *Future Med. Chem.* **2011**, *3*, 1165–1180. (c) Nishimori, I.; Minakuchi, T.; Maresca, A.; Carta, F.; Scozzafava, A.; Supuran, C. T. The  $\beta$ -carbonic anhydrases from *Mycobacterium tuberculosis* as drug targets. *Curr. Pharm. Des.* **2010**, *16*, 3300–3309.
- (4) (a) Supuran, C. T. Bacterial carbonic anhydrases as drug targets: towards novel antibiotics? *Front. Pharmacol.* **2011**, *2*, 34. (b) Winum, J. Y.; Kohler, S.; Supuran, C. T. *Brucella* carbonic anhydrases: New targets for designing anti-infective agents. *Curr. Pharm. Des.* **2010**, *16*, 3310–3316. (c) Lopez, M.; Bornaghi, L. F.; Innocenti, A.; Vullo, D.; Charman, S. A.; Supuran, C. T.; Poulsen, S. A. Sulfonamide Linked Neoglycoconjugates—A New Class of Inhibitors for Cancer-Associated Carbonic Anhydrases. *J. Med. Chem.* **2010**, *53*, 2913–2926.
- (5) (a) Švastová, E.; Hulíková, A.; Rafajová, M.; Zaťovičová, M.; Gibadulinová, A.; Casini, A.; Cecchi, A.; Scozzafava, A.; Supuran, C.;

Pastorek, J. Hypoxia activates the capacity of tumor-associated carbonic anhydrase IX to acidify extracellular pH. *FEBS Lett.* **2004**, *577*, 439–444. (b) Ebbesen, P.; Pettersen, E. O.; Gorr, T. A.; Jobst, G.; Williams, K.; Kienninger, J.; Wenger, R. H.; Pastorekova, S.; Dubois, L.; Lambin, P.; Wouters, B. G.; Supuran, C. T.; Poellinger, L.; Ratcliffe, P.; Kanopka, A.; Görlach, A.; Gasmann, M.; Harris, A. L.; Maxwell, P.; Scozzafava, A. Taking advantage of tumor cell adaptations to hypoxia for developing new tumor markers and treatment strategies. *J. Enzyme Inhib. Med. Chem.* **2009**, *24* (S1), 1–39.

(6) (a) Dubois, L.; Lieuwes, N. G.; Maresca, A.; Thiry, A.; Supuran, C. T.; Scozzafava, A.; Wouters, B. G.; Lambin, P. Imaging of CA IX with fluorescent labelled sulfonamides distinguishes hypoxic and (re)-oxygenated cells in a xenograft tumour model. *Radiother. Oncol.* **2009**, *92*, 423–428. (b) Ahlskog, J. K. J.; Dumelin, C. E.; Trüssel, S.; Marlind, J.; Neri, D. In vivo targeting of tumor-associated carbonic anhydrases using acetazolamide derivatives. *Bioorg. Med. Chem. Lett.* **2009**, *19*, 4851–4856. (c) Buller, F.; Steiner, M.; Frey, K.; Mirsof, D.; Scheuermann, J.; Kalisch, M.; Bühlmann, P.; Supuran, C. T.; Neri, D. Selection of Carbonic Anhydrase IX Inhibitors from One Million DNA-Encoded Compounds. *ACS Chem. Biol.* **2011**, *6*, 336–344. (d) Chiche, J.; Ilc, K.; Laferrère, J.; Trottier, E.; Dayan, F.; Mazure, N. M.; Brahimi-Horn, M. C.; Pouységur, J. Hypoxia-inducible carbonic anhydrase IX and XII promote tumor cell growth by counteracting acidosis through the regulation of the intracellular pH. *Cancer Res.* **2009**, *69*, 358–368. (e) Swietach, P.; Wigfield, S.; Cobden, P.; Supuran, C. T.; Harris, A. L.; Vaughan-Jones, R. D. Tumor-associated carbonic anhydrase 9 spatially coordinates intracellular pH in three-dimensional multicellular growth. *J. Biol. Chem.* **2008**, *283*, 20473–20483.

(7) (a) Supuran, C. T. Diuretics: From classical carbonic anhydrase inhibitors to novel applications of the sulfonamides. *Curr. Pharm. Des.* **2008**, *14*, 641–648. (b) De Simone, G.; Di Fiore, A.; Supuran, C. T. Are carbonic anhydrase inhibitors suitable for obtaining antiobesity drugs? *Curr. Pharm. Des.* **2008**, *14*, 655–660. (c) de Leval, X.; Iliès, M.; Casini, A.; Dogné, J. M.; Scozzafava, A.; Masini, E.; Mincione, F.; Starnotti, M.; Supuran, C. T. Carbonic anhydrase inhibitors: Synthesis and topical intraocular pressure lowering effects of fluorine-containing inhibitors devoid of enhanced reactivity. *J. Med. Chem.* **2004**, *4*, 2796–2804.

(8) (a) Sugrue, M. F. The pharmacology of antiglaucoma drugs. *Pharmacol. Ther.* **1999**, *43*, 91–138. (b) Carta, F.; Supuran, C. T.; Scozzafava, A. Novel therapies for glaucoma. A patent review 2007–2011. *Expert Opin. Ther. Pat.* **2012**, *22*, 79–88.

(9) (a) Mincione, F.; Scozzafava, A.; Supuran, C. T. The development of topically acting carbonic anhydrase inhibitors as antiglaucoma agents. *Curr. Pharm. Des.* **2008**, *14*, 649–654. (b) Mincione, F.; Scozzafava, A.; Supuran, C. T. Antiglucoma carbonic anhydrase inhibitors as ophthalmologic drugs. In *Drug Design of Zinc-Enzyme Inhibitors: Functional, Structural, and Disease Applications*; Supuran, C. T., Winum, J. Y., Eds.; Wiley: Hoboken, NJ, 2009; pp 139–154.

(10) (a) Steele, R. M.; Batugo, M. R.; Benedini, F.; Biondi, S.; Borghi, V.; Carzaniga, L.; Impagnatiello, F.; Maglietta, D.; Chong, W. K. M.; Rajapakse, R.; Cecchi, A.; Temperini, C.; Supuran, C. T. Nitric oxide-donating carbonic anhydrase inhibitors for the treatment of open-angle glaucoma. *Bioorg. Med. Chem. Lett.* **2009**, *19*, 6565–6570. (b) Mincione, F.; Benedini, F.; Biondi, S.; Cecchi, A.; Temperini, C.; Formicola, G.; Pacileo, I.; Scozzafava, A.; Masini, E.; Supuran, C. T. Synthesis and crystallographic analysis of new sulfonamides incorporating NO-donating moieties with potent antiglaucoma action. *Bioorg. Med. Chem. Lett.* **2011**, *21*, 3216–3221. (c) Fabrizi, F.; Mincione, F.; Somma, T.; Scozzafava, G.; Galassi, F.; Masini, E.; Impagnatiello, F.; Supuran, C. T. A new approach to antiglaucoma drugs: carbonic anhydrase inhibitors with or without NO donating moieties. Mechanism of action and preliminary pharmacology. *J. Enzyme Inhib. Med. Chem.* **2012**, *27*, 138–147.

(11) Supuran, C. T.; Scozzafava, A. Carbonic anhydrase inhibitors and their therapeutic potential. *Expert Opin. Ther. Pat.* **2000**, *10*, 575–600.



- (12) Liao, S. Y.; Ivanov, S.; Ivanova, A.; Ghosh, S.; Cote, M. A.; Keefe, K.; Coca-Prados, M.; Stanbridge, E. J.; Lerman, M. I. Expression of cell surface transmembrane carbonic anhydrase genes CA9 and CA12 in the human eye: overexpression of CA12 (CAXII) in glaucoma. *J. Med. Genet.* **2003**, *40*, 257–261.
- (13) (a) Kivelä, A. J.; Parkkila, S.; Saarnio, J.; Karttunen, T. J.; Kivelä, J.; Parkkila, A. K.; Pastoreková, S.; Pastorek, J.; Waheed, A.; Sly, W. S.; Rajaniemi, H. Expression of the membrane-associated carbonic anhydrase isozyme XII in the human kidney and renal tumors. *Histochem. Cell Biol.* **2000**, *114*, 197–204. (b) Hussain, S. A.; Ganesan, R.; Reynolds, G.; Gross, L.; Stevens, A.; Pastorek, J.; Murray, P. G.; Perunovic, B.; Anwar, M. S.; Billingham, L.; James, N. D.; Spooner, D.; Poole, C. J.; Rea, D. W.; Palmer, D. H. Hypoxia-regulated carbonic anhydrase IX expression is associated with poor survival in patients with invasive breast cancer. *Br. J. Cancer* **2007**, *96*, 104–109. (c) Chen, C. L.; Chu, J. S.; Su, W. C.; Huang, S. C.; Lee, W. Y. Hypoxia and metabolic phenotypes during breast carcinogenesis: Expression of HIF-1 $\alpha$ , GLUT1, and CAIX. *Virchows Arch.* **2010**, *457*, 53–61.
- (14) (a) Chia, S. K.; Wykoff, C. C.; Watson, P. H.; Han, C.; Leek, R. D.; Pastorek, J. Prognostic significance of a novel hypoxia-regulated marker, carbonic anhydrase IX, in invasive breast carcinoma. *J. Clin. Oncol.* **2001**, *19*, 3660–3668. (b) Wykoff, C. C.; Beasley, N. J.; Watson, P. H.; Turner, K. J.; Pastorek, J.; Sibtain, A.; Wilson, G. D.; Turley, H.; Talks, K. L.; Maxwell, P. H.; Pugh, C. W.; Ratcliffe, P. J.; Harris, A. L. Hypoxia-inducible expression of tumor-associated carbonic anhydrases. *Cancer Res.* **2000**, *60*, 7075–7083. (c) Bartosova, M.; Parkkila, S.; Pohlodek, K.; Karttunen, T. J.; Galbavy, S.; Mucha, V.; Harris, A. L.; Pastorek, J.; Pastorekova, S. Expression of carbonic anhydrase IX in breast is associated with malignant tissues and is related to overexpression of c-erbB2. *J. Pathol.* **2002**, *197*, 1–8.
- (15) Neri, D.; Supuran, C. T. Interfering with pH regulation in tumours as a therapeutic strategy. *Nat. Rev. Drug Discovery* **2011**, *10*, 767–777.
- (16) Ditte, P.; Dequiedt, F.; Svastova, E.; Hulikova, A.; Ohradanova-Repic, A.; Zatovicova, M.; Csaderova, L.; Kopacek, J.; Supuran, C. T.; Pastorekova, S.; Pastorek, J. Phosphorylation of carbonic anhydrase IX controls its ability to mediate extracellular acidification in hypoxic tumors. *Cancer Res.* **2011**, *71*, 7558–7767.
- (17) (a) Stillebroer, A. B.; Mulders, P. F.; Boerman, O. C.; Oyen, W. J.; Oosterwijk, E. Carbonic anhydrase IX in renal cell carcinoma: Implications for prognosis, diagnosis, and therapy. *Eur. Urol.* **2010**, *58*, 75–83. (b) Siebels, M.; Rohrmann, K.; Oberneder, R.; Stahler, M.; Haseke, N.; Beck, J. A clinical phase I/II trial with the monoclonal antibody cG250 (RENCAREX®) and interferon- $\alpha$ -2a in metastatic renal cell carcinoma patients. *World J. Urol.* **2011**, *29*, 121–126. (c) van Schaijk, F. G.; Oosterwijk, E.; Soede, A. C.; Broekema, M.; Frielink, C.; McBride, W. J. Pretargeting with bispecific anti-renal cell carcinoma x anti-DTPA(In) antibody in 3 RCC models. *J. Nucl. Med.* **2005**, *46*, 495–501.
- (18) (a) Lou, Y.; McDonald, P. C.; Oloumi, A.; Chia, S. K.; Ostlund, C.; Ahmadi, A.; Kyle, A.; Auf dem Keller, U.; Leung, S.; Huntsman, D. G.; Clarke, B.; Sutherland, B. W.; Waterhouse, D.; Bally, M. B.; Roskelley, C. D.; Overall, C. M.; Minchinton, A.; Pacchiano, F.; Carta, F.; Scozzafava, A.; Touisni, N.; Winum, J. Y.; Supuran, C. T.; Dedhar, S. Targeting Tumor Hypoxia: Suppression of Breast Tumor Growth and Metastasis by Novel Carbonic Anhydrase IX Inhibitors. *Cancer Res.* **2011**, *71*, 3364–3376. (b) Pacchiano, F.; Carta, F.; McDonald, P. C.; Lou, Y.; Vullo, D.; Scozzafava, A.; Dedhar, S.; Supuran, C. T. Ureido-substituted benzenesulfonamides potently inhibit carbonic anhydrase IX and show antimetastatic activity in a model of breast cancer metastasis. *J. Med. Chem.* **2011**, *54*, 1896–1902.
- (19) (a) Groves, K.; Bao, B.; Zhang, J.; Handy, E.; Kennedy, P.; Cuneo, G.; Supuran, C. T.; Yared, W.; Peterson, J. D.; Rajopadhye, M. Synthesis and evaluation of near-infrared fluorescent sulfonamide derivatives for imaging of hypoxia-induced carbonic anhydrase IX expression in tumors. *Bioorg. Med. Chem. Lett.* **2012**, *22*, 653–657. (b) Touisni, N.; Maresca, A.; McDonald, P. C.; Lou, Y.; Scozzafava, A.; Dedhar, S.; Winum, J. Y.; Supuran, C. T. Glycosyl coumarin carbonic anhydrase IX and XII inhibitors strongly attenuate the growth of primary breast tumors. *J. Med. Chem.* **2011**, *54*, 8271–8277.
- (20) (a) Maresca, A.; Temperini, C.; Vu, H.; Pham, N. B.; Poulsen, S. A.; Scozzafava, A.; Quinn, R. J.; Supuran, C. T. Non-zinc mediated inhibition of carbonic anhydrases: coumarins are a new class of suicide inhibitors. *J. Am. Chem. Soc.* **2009**, *131*, 3057–3062. (b) Maresca, A.; Temperini, C.; Pochet, L.; Masereel, B.; Scozzafava, A.; Supuran, C. T. Deciphering the mechanism of carbonic anhydrase inhibition with coumarins and thiocoumarins. *J. Med. Chem.* **2010**, *53*, 335–344.
- (21) Carta, F.; Temperini, C.; Innocenti, A.; Scozzafava, A.; Kaila, K.; Supuran, C. T. Polyamines inhibit carbonic anhydrases by anchoring to the zinc-coordinated water molecule. *J. Med. Chem.* **2010**, *53*, 5511–5522.
- (22) (a) Innocenti, A.; Vullo, D.; Scozzafava, A.; Supuran, C. T. Carbonic anhydrase inhibitors. Interactions of phenols with the 12 catalytically active mammalian isoforms (CA I–XIV). *Bioorg. Med. Chem. Lett.* **2008**, *18*, 1583–1587. (b) Innocenti, A.; Vullo, D.; Scozzafava, A.; Supuran, C. T. Carbonic anhydrase inhibitors. Inhibition of mammalian isoforms I–XIV with a series of substituted phenols including paracetamol and salicylic acid. *Bioorg. Med. Chem.* **2008**, *16*, 7424–742.
- (23) (a) Innocenti, A.; Scozzafava, A.; Supuran, C. T. Carbonic anhydrase inhibitors. Inhibition of cytosolic isoforms I, II, III, VII and XIII with less investigated inorganic anions. *Bioorg. Med. Chem. Lett.* **2009**, *19*, 1855–1857. (b) Innocenti, A.; Scozzafava, A.; Supuran, C. T. Carbonic anhydrase inhibitors. Inhibition of transmembrane isoforms IX, XII and XIV with less investigated inorganic anions. *Bioorg. Med. Chem. Lett.* **2010**, *20*, 1548–1550.
- (24) Temperini, C.; Scozzafava, A.; Supuran, C. T. Carbonic anhydrase inhibitors. X-Ray crystal studies of the carbonic anhydrase II—trithiocarbonate adduct—An inhibitor mimicking the sulfonamide and urea binding to the enzyme. *Bioorg. Med. Chem. Lett.* **2010**, *20*, 474–478.
- (25) Carta, F.; Aggarwal, M.; Maresca, A.; Scozzafava, A.; McKenna, R.; Supuran, C. T. Dithiocarbamates: A new class of carbonic anhydrase inhibitors. Crystallographic and kinetic investigations. *Chem. Commun. (Cambridge)* **2012**, *48*, 1868–1870.
- (26) Marzano, C.; Ronconi, L.; Chiara, F.; Giron, M. C.; Faustini, I.; Cristofori, P.; Trevisan, A.; Fregona, D. Gold(III)-dithiocarbamate anticancer agents: Activity, toxicology and histopathological studies in rodents. *Int. J. Cancer* **2011**, *129*, 487–496.
- (27) Amin, E.; Saboury, A. A.; Mansuri-Torshizi, H.; Moosavi-Movahedi, A. A. Potent inhibitory effects of benzyl and p-xylylene-bis dithiocarbamate sodium salts on activities of mushroom tyrosinase. *J. Enzyme Inhib. Med. Chem.* **2010**, *25*, 272–281.
- (28) Morpurgo, L.; Desideri, A.; Rigo, A.; Viglino, P.; Rotilio, G. Reaction of *N,N*-diethyl-dithiocarbamate and other bidentate ligands with Zn, Co and Cu bovine carbonic anhydrases. Inhibition of the enzyme activity and evidence for stable ternary enzyme-metal-ligand complexes. *Biochim. Biophys. Acta* **1983**, *746*, 168–175.
- (29) Kolayli, S.; Karahalil, F.; Sahin, H.; Dincer, B.; Supuran, C. T. Characterization and inhibition studies of an  $\alpha$ -carbonic anhydrase from the endangered sturgeon species *Acipenser gueldenstaedti*. *J. Enzyme Inhib. Med. Chem.* **2011**, *26*, 895–900.
- (30) (a) Kiran Kumar, S. T. V. S.; Kumar, L.; Sharma, V. L.; Jain, A.; Jain, R. K.; Maikhuri, J. P.; Kumar, M.; Shukla, P. K.; Gupta, G. Carbodithioic acid esters of fluoxetine, a novel class of dual-function spermicides. *Eur. J. Med. Chem.* **2008**, *43*, 2247–2256. (b) Maatschappij, B. V. Organic molybdenum compounds, use thereof as friction modifiers and lubricating compositions, W.O. Patent 113814 A1, 2008. (c) Ivanov, A. V.; Korneeva, E. V.; Gerasimenko, A. V.; Forsling, W. Structural Organization of Nickel(II), Zinc(II), and Copper(II) Complexes with Diisobutylidithiocarbamate: EPR, 13C and 15N CP/MAS NMR, and X-Ray Diffraction Studies. *Russ. J. Coord. Chem.* **2005**, *31*, 695–707. (d) Rodina, T. A.; Ivanov, A. V.; Gerasimenko, A. V.; Ivanov, M. A.; Zaeva, A. S.; Philippova, T. S.; Antzutkin, O. N. A pyridine adduct of bis(di-iso-butylidithiocarbamate-S,S')cadmium(II): Multinuclear (13C, 15N, 113Cd) CP/MAS NMR spectroscopy, crystal and molecular structure, and thermal behavior. *Inorg. Chim.*

*Acta* **2011**, *368*, 263–270. (e) Treasurywala, A. A. M.; Bagli, J.; Baker, H. Substituted pyrimidones with antifungal properties. CA Pat. 1232904, 1996. (f) Soliman, R. Dithiocarbamate esters. Part III: Synthesis and spectra of tetrahydroquinoline dithiocarbamate and xanthate esters. *Egypt. J. Chem.* **1990**, *31*, 175–186.

(31) Ivanov, A. V.; Pakusina, A. P.; Ivanov, M. A.; Sharutin, V. V.; Gerasimenko, A. V.; Antzutkin, O. N.; Groebner, G.; Forsling, W. Synthesis and single-crystal X-ray diffraction and CP/MAS 13C and 15N NMR study of tetraphenylantimony N,N-dialkyldithiocarbamate complexes: A manifestation of conformational isomerism. *Phys. Chem.* **2005**, *401*, 44–48.

(32) Khalifah, R. G. The carbon dioxide hydration activity of carbonic anhydrase. I. Stop-flow kinetic studies on the native human isoenzymes B and C. *J. Biol. Chem.* **1971**, *246*, 2561–2573.

(33) (a) Scozzafava, A.; Briganti, F.; Ilies, M. A.; Supuran, C. T. Carbonic anhydrase inhibitors Synthesis of membrane-impermeant low molecular weight sulfonamides possessing in vivo selectivity for the membrane-bound versus the cytosolic isozymes. *J. Med. Chem.* **2000**, *43*, 292–300. (b) Supuran, C. T.; Scozzafava, A.; Ilies, M. A.; Briganti, F. Carbonic anhydrase inhibitors. Synthesis of sulfonamides incorporating 2,4,6-trisubstituted-pyridinium-ethylcarboxamido moieties possessing membrane-impermeability and in vivo selectivity for the membrane-bound (CA IV) versus the cytosolic (CA I and CA II) isozymes. *J. Enzyme Inhib.* **2000**, *15*, 381–401.

(34) (a) Alterio, V.; Di Fiore, A.; D'Ambrosio, K.; Supuran, C. T.; De Simone, G. X-Ray crystallography of CA inhibitors and its importance in drug design. In *Drug Design of Zinc-Enzyme Inhibitors: Functional, Structural, and Disease Applications*; Supuran, C. T., Winum, J. Y., Eds.; Wiley: Hoboken, 2009; pp 73–138. (b) Alterio, V.; Hilvo, M.; Di Fiore, A.; Supuran, C. T.; Pan, P.; Parkkila, S.; Scaloni, A.; Pastorek, J.; Pastorekova, S.; Pedone, C.; Scozzafava, A.; Monti, S. M.; De Simone, G. Crystal structure of the extracellular catalytic domain of the tumor-associated human carbonic anhydrase IX. *Proc. Natl. Acad. Sci. U.S.A.* **2009**, *106*, 16233–16238.

(35) (a) Casini, A.; Antel, J.; Abbate, F.; Scozzafava, A.; David, S.; Waldeck, H.; Schafer, S.; Supuran, C. T. Carbonic anhydrase inhibitors: SAR and X-ray crystallographic study for the interaction of sugar sulfamates/sulfamides with isozymes I, II and IV. *Bioorg. Med. Chem. Lett.* **2003**, *13*, 841–845. (b) De Simone, G.; Di Fiore, A.; Menchise, V.; Pedone, C.; Antel, J.; Casini, A.; Scozzafava, A.; Wurl, M.; Supuran, C. T. Carbonic anhydrase inhibitors. Zonisamide is an effective inhibitor of the cytosolic isozyme II and mitochondrial isozyme V: solution and X-ray crystallographic studies. *Bioorg. Med. Chem. Lett.* **2005**, *15*, 2315–2320. (c) Temperini, C.; Innocenti, A.; Scozzafava, A.; Parkkila, S.; Supuran, C. T. The coumarin-binding site in carbonic anhydrase accommodates structurally diverse inhibitors: The antiepileptic lacosamide as an example. *J. Med. Chem.* **2010**, *53*, 850–854.

(36) (a) Avvaru, B. S.; Wagner, J. M.; Maresca, A.; Scozzafava, A.; Robbins, A. H.; Supuran, C. T.; McKenna, R. Carbonic anhydrase inhibitors. The X-ray crystal structure of human isoform II in adduct with adamantyl analogue of acetazolamide resides in a less utilized binding pocket than most hydrophobic inhibitors. *Bioorg. Med. Chem. Lett.* **2010**, *20*, 4376–4381. (b) Wagner, J. M.; Avvaru, B. S.; Robbins, A. H.; Scozzafava, A.; Supuran, C. T.; McKenna, R. Cumarinyl-substituted sulfonamides strongly inhibit several human carbonic anhydrase isoforms: solution and crystallographic investigations. *Bioorg. Med. Chem.* **2010**, *18*, 4873–4878. (c) Pacchiano, F.; Aggarwal, M.; Avvaru, B. S.; Robbins, A. H.; Scozzafava, A.; McKenna, R.; Supuran, C. T. Selective hydrophobic pocket binding observed within the carbonic anhydrase II active site accommodate different 4-substituted-ureido-benzenesulfonamides and correlate to inhibitor potency. *Chem. Commun. (Cambridge)* **2010**, *46*, 8371–8373.

(37) McPherson, A. *Preparation and Analysis of Protein Crystals*, 1st ed.; Wiley: New York, 1982.

(38) Otwinowski, Z.; Minor, W. Processing of x-ray diffraction data collected in oscillation mode. *Methods Enzymol.* **1997**, *276*, 307–326.

(39) Avvaru, B. S.; Kim, C. U.; Sippel, K. H.; Gruner, S. M.; Agbandje-McKenna, M.; Silverman, D. N.; McKenna, R. A short,

strong hydrogen bond in the active site of human carbonic anhydrase II. *Biochemistry* **2010**, *49*, 249–251.

(40) Adams, P. D.; Afonine, P. V.; Bunkóczi, G.; Chen, V. B.; Davis, I. W.; Echols, N.; Headd, J. J.; Hung, L.-W.; Kapral, G. J.; Grosse-Kunstleve, R. W.; McCoy, A. J.; Moriarty, N. W.; Oeffner, R.; Read, R. J.; Richardson, D. C.; Richardson, J. S.; Terwilliger, T. C.; Zwart, P. H. PHENIX: A comprehensive Python-based system for macromolecular structure solution. *Acta Crystallogr.* **2010**, *D66*, 213–221.

(41) Brunger, A. T. Free R value: A novel statistical quantity for assessing the accuracy of crystal structures. *Nature* **1992**, *355*, 472–475.

(42) Emsley, P.; Cowtan, K. Coot: Model-building tools for molecular graphics. *Acta Crystallogr., Sect. D* **2004**, *D60*, 2126–2132.

(43) Laskowski, R. A.; MacArthur, M. W.; Moss, D. S.; Thornton, J. M. PROCHECK: A program to check the stereochemical quality of protein structures. *J. Appl. Crystallogr.* **1993**, *26*, 283–291.